



UNIVERSITY OF LEEDS

This is a repository copy of *A visual indicator based on curcumin with high stability for monitoring the freshness of freshwater shrimp, Macrobrachium rosenbergii*.

White Rose Research Online URL for this paper:
<https://eprints.whiterose.ac.uk/180560/>

Version: Accepted Version

Article:

Zhang, J, Huang, X, Zou, X et al. (8 more authors) (2021) A visual indicator based on curcumin with high stability for monitoring the freshness of freshwater shrimp, *Macrobrachium rosenbergii*. *Journal of Food Engineering*, 292. 110290. ISSN 0260-8774

<https://doi.org/10.1016/j.jfoodeng.2020.110290>

© 2020 Elsevier Ltd. All rights reserved. This manuscript version is made available under the CC-BY-NC-ND 4.0 license <http://creativecommons.org/licenses/by-nc-nd/4.0/>.

Reuse

This article is distributed under the terms of the Creative Commons Attribution-NonCommercial-NoDerivs (CC BY-NC-ND) licence. This licence only allows you to download this work and share it with others as long as you credit the authors, but you can't change the article in any way or use it commercially. More information and the full terms of the licence here: <https://creativecommons.org/licenses/>

Takedown

If you consider content in White Rose Research Online to be in breach of UK law, please notify us by emailing eprints@whiterose.ac.uk including the URL of the record and the reason for the withdrawal request.



eprints@whiterose.ac.uk
<https://eprints.whiterose.ac.uk/>

22 increased elongation at break of hydrogel films from 47.02% to 68.69% but reduced
23 their water content. The curcumin film showed a greater colorimetric stability at 4 °C
24 which ΔE value was 3.93. The hydrogel films exhibited obvious color changes to
25 ammonia while the electrochemical writing pattern was well-stable acts as a reference.
26 Meanwhile, the intelligent indicator presented a highly color change from yellow to red
27 with the increasing of shrimp storage time. Last but not the least, the printed
28 information not only provides the basic information of packaging (production date,
29 shelf-life, etc.) but also has the reference function for an indicator.

30 **Keywords: curcumin; hydrogel film; shrimp; electrochemical writing; color**
31 **stability; non-destructive method**

32 **1. Introduction**

33 *Macrobrachium rosenbergii* is one of the most economically important freshwater
34 shrimps with fast growth and high fecundity in agricultural development on a global
35 scale (Li et al., 2019). However, *Macrobrachium rosenbergii* is susceptible to
36 contamination by bacteria and mildew triggering rapid death and severe economic
37 losses (Soares et al., 2013). Therefore, it is indispensable to monitor its freshness for
38 better health protection of the consumers. Generally, the decomposition of protein in
39 *Macrobrachium rosenbergii* produces various volatile nitrogenous compounds such as
40 ammonia, dimethylamine, and trimethylamine (Zhang et al., 2019). Then the total
41 volatile basic nitrogen (TVB-N) level is increasing and bringing alteration to the pH of

42 packaging environment. Recently, the visual pH indicators for food freshness attract
43 widespread attention. Novel pH indicators have been developed for ‘on-package’ which
44 can track food quality in real time by naked eyes without any sample destruction (Choi
45 et al., 2017; Huang et al., 2019). Likewise, the color of curcumin shows visual change
46 from yellow to orange-red with the pH increasing (Liu et al., 2018). Curcumin, which
47 exhibits antiviral, antimicrobial, antioxidant, and anticancer properties, is a natural dye
48 comprising of a dike tone compound extracted from the *Curcuma* rhizomes (Pereira
49 and Andrade, 2017). Nowadays, several works have reported the use of curcumin as a
50 pH indicator to indicate food spoilage (Luo et al., 2012; Musso et al., 2016; Ma et al.,
51 2017a). For instance, an indicator film was developed based on κ -carrageenan and
52 curcumin to monitor the freshness of pork and shrimp samples (Liu et al., 2018).

53 Previously, in order to immobilize natural pH dyes, several film-forming materials
54 such as polyvinyl alcohol, chitosan and agar have been prepared (Mannozi et al., 2018;
55 Ebrahimi Tirtashi et al., 2019). Agar is extracted from Gelidiaceae and Gracilariaceae
56 families of seaweeds and has well-defined phase barriers in the gel-forming process.
57 Polyvinyl alcohol (PVA) is a synthetic vinyl polymer with a C-C chain backbone and
58 polyhydroxyl. The hydroxyl groups in PVA may cause high solubility and weak water
59 resistance. Thus, it is imperative to incorporate PVA with another natural polymer that
60 could enhance its physical properties (Lyons et al., 2009).

61 The traditional inks used for printing are usually toxic which limits their suitability
62 for food products. Therefore, a new method about ink-free printing on hydrogel films

63 fetches the attention of food industries. Previous work reported that printing on chitosan
64 and agarose film has provided valuable information about fish freshness with
65 electrochemistry analysis (Wu et al., 2018). Besides, Zhai and co-workers have
66 developed an edible film combined with electrochemical writing for milk and carp
67 freshness (Zhai et al., 2018). However, as the mentioned indicators above, they showed
68 lower stability owing to the degradation of the anthocyanins which directly related to
69 the coloration of the indicators (Kara and Erçelebi, 2013). Therefore, in our study, the
70 curcumin was used as the pH dye, and agar was bound with PVA as the film-forming
71 materials to prepare the hydrogel film indicator. And we aimed to provide a
72 multifunction curcumin indicator. The ink-free printed information not only provides
73 the basic information on packaging (production date, shelf-life, etc.) but also has the
74 reference function. This indicator was similar as a ratio indicator, the curcumin film
75 was used as a sensor for meat freshness and the imprinted character was used as a
76 reference. Interestingly, the imprinted was written on the hydrogel film based on
77 electrochemical analyzer and a robotic arm was provided for an assistant device of an
78 automatic ink-free printing method.

79 **2. Material and Methods**

80 **2.1 Materials**

81 Shrimp (*Macrobrachium Rosenbergii*) was purchased from the local supermarket
82 in Zhenjiang city of Jiangsu province, China. Polyvinyl alcohol (molecular weight
83 about 77000) and agar were acquired from Shanghai Natural Wild-insect Kingdom Co.,

84 Ltd. Glycerin (EG, 99.9%) and Ethyl alcohol ($\geq 99.5\%$) were obtained from Sinopharm
85 Chemical Reagent Co., Ltd (Shanghai, China). Curcumin powders were purchased
86 from Macklin Biochemical Co., Ltd (Shanghai, China). Disodium citrate was purchased
87 from Jiangsu Thorpe Group Co. Ltd (Jiangsu, China). Buffers with the pH range of 3.0-
88 11.0 were acquired with citric acid/disodium hydrogen phosphate. Glass molds were
89 acquired from Sigma Chemical Co. Ltd (St. Louis, MO, USA).

90 **2.2 Preparation of hydrogel films**

91 The hydrogel films were prepared following a series of processes. Firstly, 100 mL
92 of distilled water containing 1.6 g agar and 0.4 g PVA (AP) was heated and stirred with
93 a magnetic stirrer (F-101S, YUHUA, China) at 100 °C for 60 minutes (Lyons et al.,
94 2009). Afterward, the curcumin with different concentrations (0-3% of the AP, w/w)
95 was dissolved in a series of ethanol solutions (5 mL, ethanol/water = 4:1, v:v). Then,
96 the mixture was added to the AP solution at 60 °C expressed as CAP1, CAP2, and CAP3,
97 respectively. The mixed solution was stirred until it was utterly homogenized. Each
98 hydrogel film was prepared by casting 10 g of mixing solution into a smooth glass mold
99 (90×90 mm) at room temperature for 10 minutes. The prepared hydrogel films were
100 stored at 4 °C for further analysis.

101 **2.3 UV-Vis spectroscopy measurement**

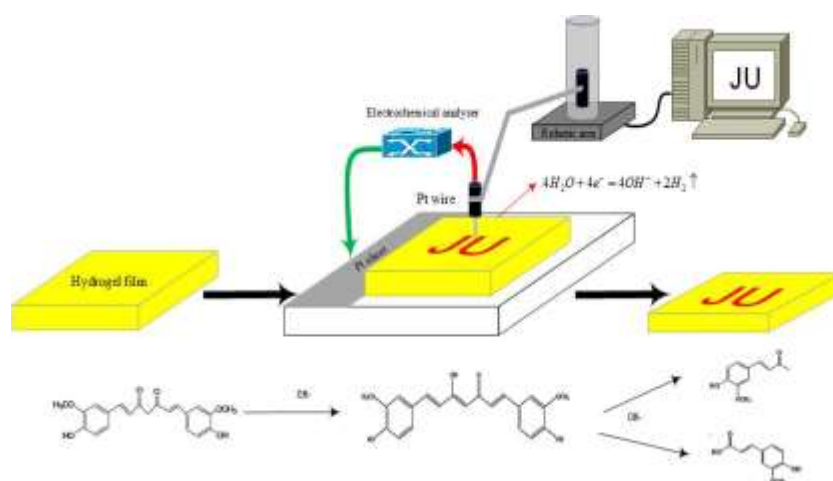
102 The UV-Vis spectra of curcumin in the range of pH 3.0-11.0 was measured using
103 an Agilent CARY 100 UV-Vis spectrophotometer (Varian Corporation, USA). The
104 absorbance of solutions was measured in the range of 400-800 nm and the solution

105 without curcumin was served as blank.

106 2.4 Electrochemical writing on hydrogel films.

107 The cathode made of a platinum wire counter electrode (diameter 0.5 mm)
108 contacted onto the surface of the hydrogels and the anode (platinum sheet)
109 underside of the hydrogel. The constant applied voltage was set at -10V, then OH⁻ was
110 produced at the cathode. With the increasing of the local pH, the color of the imprinted
111 characters changed from yellow to red at the cathode. As shown in Fig. 1, the moving
112 cathode on the hydrogel was controlled by a robotic arm (Yue Jiang Technology Co.,
113 Ltd., Shenzhen, China). The required characters or motifs were printed by
114 electrochemical writing and controlled by an in-built computer program attached to the
115 system. In this study, the characters “JU” (Jiangsu University) were printed on hydrogel
116 films and the size of the letter was controlled to 25.66×17.00 mm. Finally, the hydrogel
117 film was dried with excess water being evaporated in an oven at 50 °C for 6 h.

118



119 **Fig. 1.** Schematic diagram of electrochemical printing

120

121 **2.5 Characteristics of the hydrogel films**

122 **2.5.1 Morphology and structure of hydrogel films**

123 Fourier transform infrared (FT-IR) spectra of the hydrogel films with different
124 curcumin concentrations were carried out on a Nicolet 50 infrared spectrometer (Boston,
125 USA). The spectra were acquired at a resolution 4 cm^{-1} in the range of 4000 and 650
126 cm^{-1} with the ATR mode and three scans. Then, the cross-section of hydrogel films was
127 examined by a scanning electron microscopy (SEM, JSM-7800F, Japan electronics,
128 Japan). Prior to analysis, the samples were dried, and then attached onto the slide of
129 aluminum stubs. All of the samples were coated with a thin layer of gold under vacuum
130 at an accelerating voltage of 15 kV.

131 **2.5.2 The physical characteristics of hydrogel films.**

132 The thickness of the hydrogel films was recorded by a digital micrometer (Sanfeng
133 Group Co., Taiwan, China). The tensile strength (TS) and elongation at break (EB) were
134 measured using a universal texturometer (Model 4500, Instron Corporation, Canton,
135 MA, USA) according to the method of ASTM D882-00. Prior to analysis analysis, each
136 film was cut into 60 mm length and 20 mm width. The crosshead speed was set to 0.06
137 mm/s and the initial grip separation was set to 40 mm with 150 kg of a load cell.

138 The water content (WC) of hydrogel films was measured by moisture drying
139 method at $105\text{ }^{\circ}\text{C}$ according to the following equation:

$$140 \quad WC (\%) = 100 \times (M_i - M_f) / M_i \quad (1)$$

141 Where M_i was the initial weight of hydrogel (g) and M_f was the final weight of

142 hydrogel at 105 °C (g).

143 2.5.3 The stability of curcumin film and the electro-writing with letter “JU”

144 The hydrogel films were stored in an incubator at 4 and 25 °C with 75% relative
145 humidity (RH). The color of films was determined by using a Scanjet G4050 optical
146 scanner (HP, China) for two weeks. The stability of the curcumin film and the imprinted
147 characters “JU” were both defined as the color change based on the following equations:
148 Lab model is a kind of color pattern published by the International Commission on
149 illumination (CIE) in 1976. Lab mode is also composed of three channels. The value of
150 L^* is the lightness, a^* is red to green, and b^* is yellow to blue.

$$151 \quad \Delta E = \sqrt{(\Delta L^*)^2 + (\Delta a^*)^2 + (\Delta b^*)^2} \quad (2)$$

152 Where $\Delta L^* = L^* - L_0^*$; $\Delta a^* = a^* - a_0^*$; $\Delta b^* = b^* - b_0^*$; L_0^* , a_0^* and b_0^* were the initial color
153 values of the films, L^* , a^* and b^* were the color after storage.

154 2.6 The sensitivity of hydrogel films to ammonia.

155 The response of the hydrogel films to ammonia was determined according to the
156 method described by Kuswandia (Kuswandia et al., 2012) with slight modification. The
157 hydrogel films were cut into squares then sealed on the conical flask (500 mL) by a
158 rubber band containing ammonia for 24 minutes at room temperature. The
159 concentration of the ammonia was 100 mmol/L. An image was captured by the camera
160 which fixed on the top of the light box (50×50×50 cm) every 2 minutes (Fig. S1). On
161 both sides of the light box, there are two fluorescent lights with a fixed position, incident
162 angle and intensity kept (details in the Supplementary material). Then the R, G, B of

163 the picture of films were obtained by using the MATLAB (Version 2013, Math Works,
164 USA). The response sensitivity (S) of the hydrogel films was calculated according to
165 the following equations (Huang et al., 2015; Zhai et al., 2018):

$$166 \quad \Delta R = |R_a - R_b|$$

$$167 \quad \Delta G = |G_a - G_b|$$

$$168 \quad \Delta B = |B_a - B_b| \tag{3}$$

$$169 \quad S = \frac{\Delta R + \Delta G + \Delta B}{R_b + G_b + B_b} \times 100\%$$

170 where R_a , G_a , B_a were the initial values of the red, green and blue, R_b , G_b , B_b were the
171 color of detection under ammonia

172 **2.7 The application test of hydrogel films for shrimp**

173 **2.7.1 Gas chromatography-mass spectrometer (GC-MS) analysis**

174 Before the GC-MS analysis, the shrimp samples were homogenized into mince
175 and then pretreated by Solid-phase micro-extraction (SPME). The samples of 6 g
176 minced shrimp were put into the extraction bottle (15 mL). A screw cup and silicone
177 septum were on the extraction bottle to make it airtight (ANPEL Laboratory
178 Technologies Inc., Shanghai, China). The samples were equilibrated for 10 minutes at
179 60 °C. Then the volatiles were extracted for 20 minutes at 60 °C onto the SPME fiber
180 assembly (50/30 μm DVB/CAR/PDMS, 1 cm, gray; ANPEL Laboratory Technologies
181 (Shanghai) Inc.).

182 These volatile nitrogenous compounds were detected using the Trace Ultra
183 ITQ1100 GC-MS system (Thermo Scientific, Waltham, MA). After extraction, the

184 fiber desorbed the splitless into the GC injector at 250 °C for 5 minutes. The separation
185 was carried out by using a column Agilent DB-WAX (60 m length×0.25 mm I.D.×0.25
186 um film thicknesses; Agilent Technologies, Folsom, CA, USA) with a gas Helium flow
187 rate of 1 mL/min. The initial temperature program was set at 40 °C with 4 minutes and
188 then warmed to 100 °C with 10 °C/min, finally followed by a ramp of 6 °C/min to
189 220 °C and then held for 3 minutes. The MS spectrometer was set at -70 eV electron
190 energy with ion source setting at 230 °C by the Agilent 5973 MSD. The temperature
191 for quadrupole was set at 200 °C. The identification of the volatile nitrogenous
192 compounds was compared to the mass spectra with National Institute of Standards and
193 Technology (NIST) library (Zhai et al., 2019).

194 **2.7.2 The shrimp spoilage trial**

195 The hydrogel film indicator was used to evaluate the freshness of the shrimp.
196 Firstly, 50 g of shrimp samples were placed into a crisper with a CAP2 film indicator
197 fixing on it. The size of each hydrogel film has a diameter of 40 mm. The crisper box
198 was placed at 4 °C and 75% RH. The film was captured every 12 hours for three days
199 with a CR-400 portable Chromameter (KONICA MINOLTA, Japan). The TVB-N of
200 shrimp was measured according to the method described by the semi-micro *Kjeldahl*
201 method (Zhang et al., 2019).

202 **2.8 Statistical analysis**

203 All the analyses were performed in triplicate independent experiments and
204 reported as average ± std. Mean differences on a completely randomized design were

205 performed with the analysis of variance (ANOVA) procedure in Statistic Package for
206 Social Science (SPSS) software (Version 21, SPSS Inc) followed by Duncan's multiple
207 range test for mean comparison. The significance was defined to be at a P value of less
208 than 5%.

209 **3. Results and discussion**

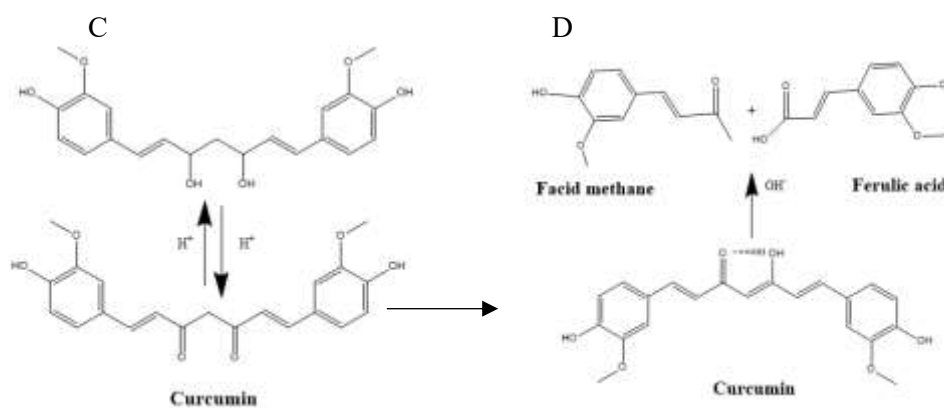
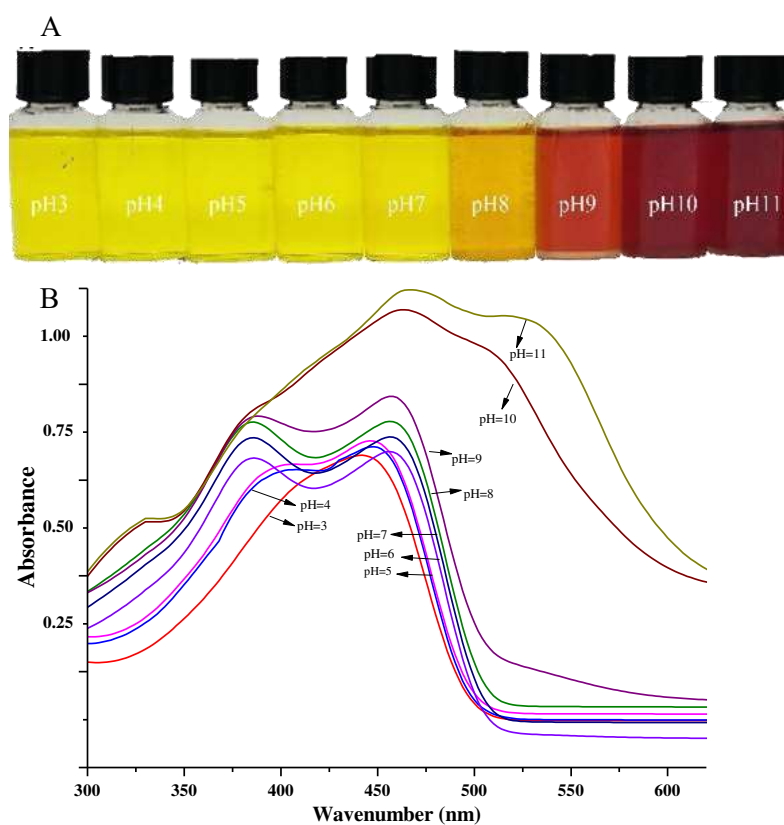
210 **3.1 UV-vis spectra and color of curcumin**

211 The color of curcumin and UV-vis spectra are shown in Fig. 2. As can be seen, the
212 Fig. 2A demonstrates a noticeable change of curcumin color from light yellow to
213 orange-red as the pH values increased from 3.0 to 11.0. Curcumin was light yellow
214 when the pH was less than 5.0, yellow-orange at pH 6.0-7.0, and reddish-orange at pH
215 10.0-11.0. The changes assigned to the phenolic compounds and unsaturated bonds
216 structure of curcumin (Rupesh Kumar et al., 2011). Thus, Fig. 2B shows that the
217 absorption peak of curcumin was at about 448 nm (pH<5). With increasing pH, the
218 maximum absorption peak shifts to 462 nm and another new absorption peak produced
219 at 388 nm in the range of pH 6.0-9.0. Similar pH-sensitive color changes of curcumin
220 were observed by Liu et al., 2018. Under acidic conditions, the variation of curcumin
221 peak location depended on its chemical structure. It has two distinct structures, one
222 exists in an enol form the other presence of the diketone (Fig. 2C). As alkalinity further
223 increasing, the intramolecular charge transferred from the phenyl ring towards the
224 carbonyl and changed the moiety diketone structure of curcumin (Zsila et al., 2003).
225 The electronegativity was enhanced to produce a dark effect, causing the changes in

226 maximum absorption wavelength and intensity (Hazzah et al., 2015). Moreover, a
 227 significant change in the spectra was observed in the range of 10.0-11.0, showing two
 228 new absorption peaks at 336 nm and 464 nm. These new peaks were probably caused
 229 by the degradation of curcumin to ferulic acid and its methane forms (Fig. 2D).

230

231



233 **Fig. 2.** (A) Colors, and (B) UV-vis spectra of curcumin solutions at pH 3–11; (C) structure of
234 curcumin in acidic conditions (D) degrades of curcumin in alkaline conditions

235

236

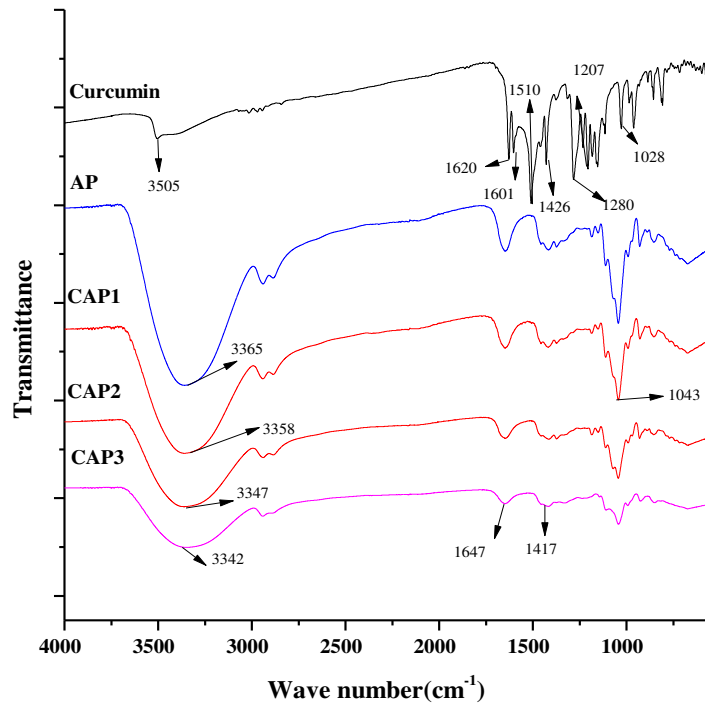
237 **3.2 Characterization of the hydrogel films**

238 **3.2.1 Morphology and structure of films**

239 Fig. 3 illustrates the FT-IR spectra of curcumin powders, AP, CAP1, CAP2, and
240 CAP3 films. The peaks of the curcumin spectrum at 3505 cm^{-1} , 1620 cm^{-1} and 1601
241 cm^{-1} were ascribed to the free vibration of -OH phenolic stretching, C=O stretching and
242 C-H bending bound to methyl groups, respectively (Mohan et al., 2012; Mangolim et
243 al., 2014). The bands located at 1501 cm^{-1} and 1280 cm^{-1} corresponding to stretching
244 vibrations of C=C and C=O of aromatic rings (Silva-Pereira et al., 2015). The bands
245 presented at 1207 cm^{-1} , 1426 cm^{-1} and 1028 cm^{-1} were assigned to stretching vibrations
246 of C-C, C-O and C-O-C bending (Zhou and Tang, 2016). The spectra of hydrogel films
247 were characterized in the dehydrated state of the hydrogel film. A shift in the spectral
248 region with an increased intensity of 1043 cm^{-1} was described to a C-C stretching mode
249 of PVA crystallinity. The intense peaks at 1647 cm^{-1} and 1417 cm^{-1} were associated with
250 C=C stretching of the phenyl ring. Furthermore, the peaks around the -OH stretching
251 vibration at 3365 cm^{-1} moved to 3358 cm^{-1} , 3347 cm^{-1} and 3342 cm^{-1} with the addition
252 of curcumin from 0, 1, 2, and 3% of the AP, respectively. Also, the intensity decreased
253 with the curcumin solution increasing. These results were probably assigned to the
254 hydrogen bonding interaction between the agar/PVA matrix and curcumin. Curcumin is

255 a hydrophobic active component and the addition of curcumin weakened the hydrogen
256 bonding interaction (Wang et al., 2016).

257



258

259 **Fig. 3.** FTIR of curcumin and hydrogel films with Curcumin contents at: 0%, 1%, 2%, 3%.

260

261

262

263 The cross-section of AP, CAP1, CAP2 and CAP3 films by SEM are shown in Fig.

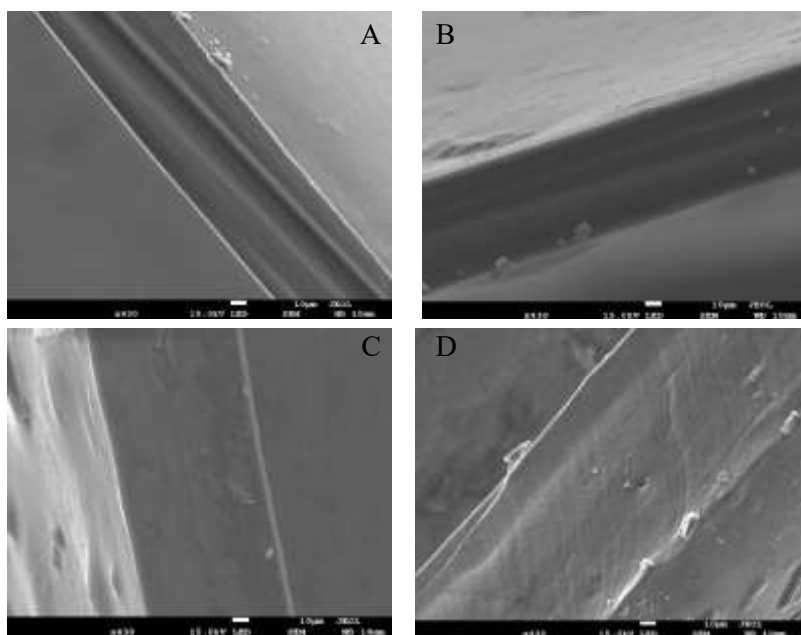
264 4. The AP film exhibited excellent compatibility which has a smooth and flat surface.

265 The results indicated that film-forming materials have no apparent phase separation as

266 shown in Fig. 4A. After the addition of curcumin, the micro-phase of CAP1 film was

267 well distributed. However, the curcumin crystal distribution in the surface of CAP2 film

268 deteriorated and the structure was not as smooth as AP and CAP1. The structure showed
269 typical irregularities associated with the hemimorphic crystals form (Cano et al., 2015).
270 The curcumin crystals became more poorly distributed and precipitated with the
271 increasing concentration of curcumin. The amorphous phases of CAP3 film showed the
272 least favorable structure with evident agglomeration as illustrated in Fig. 4D.
273 Meanwhile, the whole cross-section presented irregularities in a crystalline structure
274 which was caused by decreasing solubility promoting crystal formation. As a result,
275 low curcumin content may be well-distributed in the film-forming materials, but higher
276 curcumin content is related to a high degree of crystallinity. The phenomenon was
277 consistent with the observation made by Liu et al.



278

279 **Fig. 4.** SEM images of hydrogel films: AP (A), CAP1 (B), CAP2 (C), and CAP3 (D)

280

281

282 3.2.2 The physical characteristics of hydrogel films

283 The thickness, TS, EB and WC of hydrogel films are shown in Table S1. The
284 results obviously indicate that the thickness of the hydrogel films slightly increases with
285 the addition of curcumin content. The increasing content of curcumin changed the
286 interior structure of the hydrogel-forming matrix and the increasing in the spatial
287 distance between curcumin and the polymer film-forming material (Liu et al., 2016).
288 WC was investigated to evaluate the water resistance of the packaging films. The WC
289 of CAP film decreased significantly compared to the control film ($p < 0.05$), of which
290 values decreased from 42.99% to 40.73%, 27.25% and 12.20% with the concentration
291 of curcumin from 0% to 3% of AP, respectively. The altered WC of CAP film may have
292 been caused by the hydrophobicity of curcumin. In addition, the molecular interaction
293 between the base materials and the curcumin of hydroxyl groups was a possible barrier
294 to moisture diffusion through the CAP films (Musso et al., 2016). Generally, the
295 addition of active compounds can decrease the TS of films because of the weakened
296 interaction between film-forming materials and curcumin (small molecule compound)
297 (Noronha et al., 2014). However, the TS of CPA3 film was higher than the CAP1 film
298 because of film discontinuities, but it was still lower than the AP (control film). It can
299 also be seen that the EB of hydrogel films increases from 47.02% to 62.91%, 66.52%
300 and 68.69% with the concentration of curcumin from 0% to 3% of AP, respectively.
301 Therefore, these behaviors of films were due to the following two reasons: the curcumin

302 into the agar/PVA matrix increased the polymer mobility and hydrogen bond interaction
303 (Luo et al., 2012).

304 Table S1 Summary of the mechanical properties of CAP films.

Samples	Film thickness (mm)	TS (MPa)	EB (%)	WC (%)
AP	0.087 ± 0.007 ^b	7.54 ± 0.54 ^a	47.02 ± 0.83 ^c	42.99 ± 2.61 ^a
CAP1	0.093 ± 0.002 ^b	4.38 ± 0.08 ^b	62.91 ± 1.42 ^b	40.73 ± 1.28 ^a
CAP2	0.104 ± 0.001 ^a	5.22 ± 0.49 ^b	66.52 ± 1.19 ^a	27.25 ± 2.84 ^b
CAP3	0.106 ± 0.001 ^a	6.94 ± 0.14 ^a	68.69 ± 0.50 ^a	12.20 ± 1.28 ^c

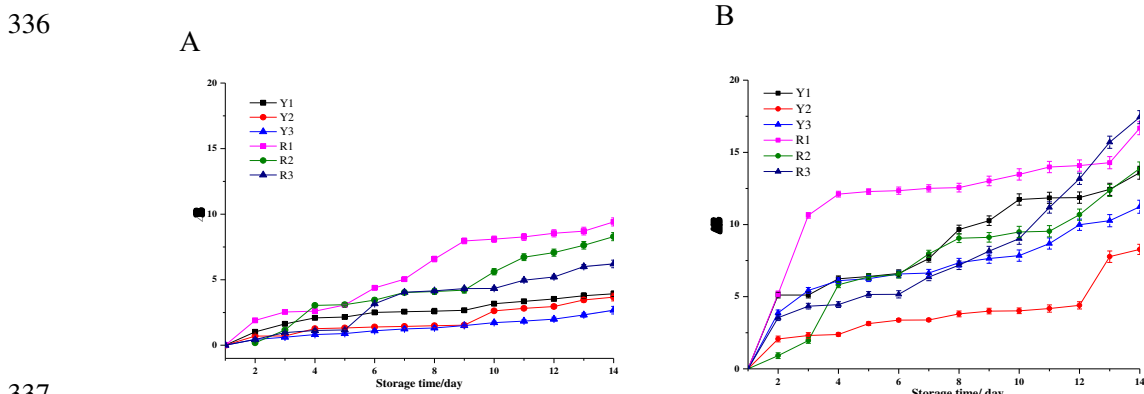
306 Notes: data with the same superscript letter in the same column indicate that statistically different ($p < 0.05$). The data (mean ± standard) result from three
307 replicates. Where: TS: tensile strength; EB: elongation at break; WC: water content

308
309
310

311 3.2.3 The stability of hydrogel films

312 The color stability of curcumin films and the imprinted characters “JU” was a
313 crucial role of the color performance in relation to freshness detection. The color
314 variations of curcumin films and the characters “JU” are shown in Fig. 5. Compared to
315 the color of imprinted characters, the curcumin films showed a higher stability.
316 Generally, the imprint character region was produced due to the OH⁻ at the cathode
317 (Electrochemical Writing) and then the phenol hydroxyl groups easily converted to a
318 phenolic oxygen anion of curcumin. Besides that, the localized curcumin was more
319 easily oxidized and reduced the stability of the imprint characters (Zhai et al., 2018).
320 Fig. 5A shows that the curcumin films stored at 4 °C had lower ΔE values which was
321 3.93 at the 14th day, indicating that they had more excellent color stability. By contrast,
322 the color of the curcumin films changed for two weeks at a higher temperature (25 °C).
323 The more inferior stability of curcumin was due to oxidization reaction at a higher

324 temperature (Ma et al., 2017b). The difference was also recorded by the color stability
 325 between the different content of curcumin in the hydrogel films. It can be seen that the
 326 color stabilities of the curcumin films and the imprint character “JU” both improved
 327 with the increase of curcumin content. The results indicated that the hydrogel films with
 328 more curcumin content possessing higher color stabilities at 4 °C. The hydrophobic of
 329 the curcumin modified the retention of active ingredients in hydrogel films. Hence, the
 330 phenolic hydroxyl group of hydrogel films with high curcumin concentration could not
 331 be readily formed into phenoxide anion (Musso et al., 2017). However, there was no
 332 similar pattern found at 25 °C. The irregular change of ΔE values was related to the
 333 accelerated polymer mobility of curcumin at a higher temperature (Kuorwel et al.,
 334 2013). The instability of indicators at high temperature has been shown as the previous
 335 studies (Zhang et al., 2019;Huang et al., 2019; Mohammadalinejhad et al., 2020).



337
 338 **Fig. 5.** The relative color change (ΔE values) of the hydrogels stored at (A) 4 °C, (B)
 339 25 °C for 14 days;

340 Where: Y1: CAP1; Y2: CAP2; Y3: CAP3; R1: Red letter of CAP1; R2: Red letter of
 341 CAP2; R3: Red letter of CAP3
 342

343 3.2.4 Sensitivity of hydrogel films to ammonia

344 In order to evaluate the sensor function of the hydrogel films, the curcumin films
345 were exposed in an ammonia environment. As shown in Fig. 6, the curcumin films
346 presented visible response sensitivity to ammonia at different response times. However,
347 the character imprint “JU” had small response sensitivity within 24 minutes. Curcumin
348 showed a strong redness-shift under the alkaline condition, the redness color was
349 enhanced with the increase of reaction time. The decomposition of curcumin was
350 accelerated in the alkaline concentration. Meanwhile, the phenoxide anion was easily
351 formed and produced the color changes (Ma et al., 2017a). It can be seen that the S
352 values of films improved with the increase of curcumin content. According to the
353 sensitivity test to ammonia, the curcumin film was used as a sensor for shrimp freshness
354 and the imprint character was used as a reference.

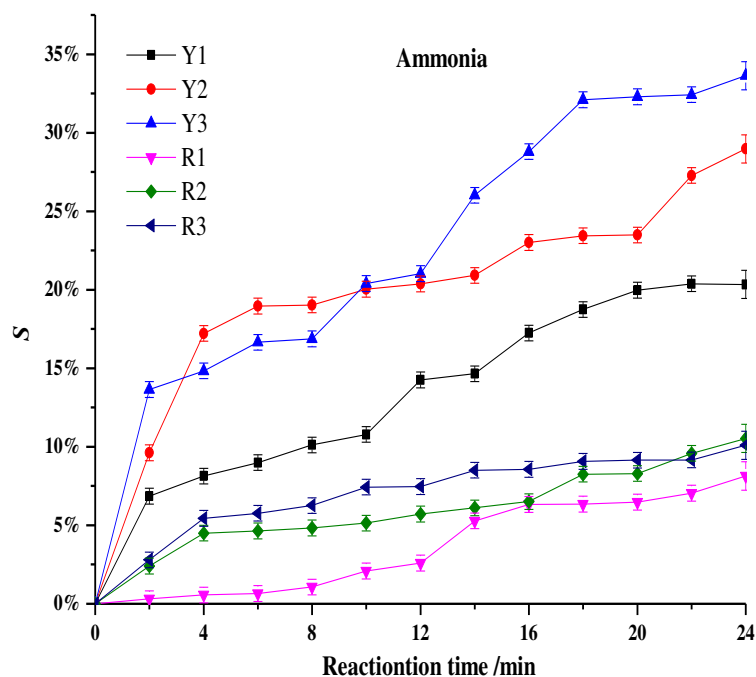


Fig. 6. The color response of the curcumin film and the letter “JU” toward ammonia gas.

3.3 Application of hydrogel films to shrimp

The CAP2 hydrogel film was employed to monitor the shrimp freshness due to its excellent mechanical properties and higher color variation rate. The curcumin film presented visible S values while the imprint character did not show significantly change in the ammonia environment. Therefore, the curcumin film was used as a sensor for shrimp freshness and the imprinted character was used as a reference. As shown in Fig. 7A, the curcumin film gradually changed from yellow to orange-red with the decline of shrimp freshness. By SPME/GC-MS analysis, the Table S2 shows that volatile compounds contents of the freshness sample have a little amount. Only six compounds were produced in the first day of the *Macrobrachium Rosenbergii* and there were no

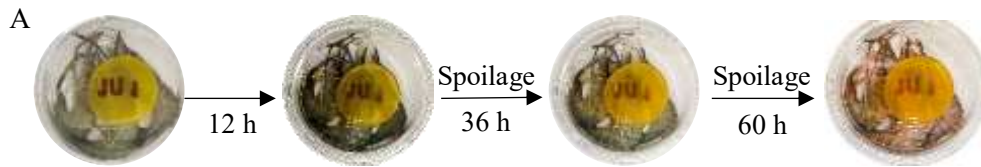
369 decomposition odors in the freshness sample. While as shown in Table S3, abundant
370 compounds approximately eighteen were identified in the spoiled sample after the
371 storage time of shrimp. And the results indicated that the most obvious compounds were
372 trimethylamine, 2-Octanol and phenol in a spoiled sample. The results were
373 corresponding to the detections of the TVB-N levels (Zhang et al., 2019). The TVB-N
374 values of shrimp increased from 8.7 to 18.6 mg/100 g at 24 h. According to the Chinese
375 standard GB2733-2015, the limit of TVB-N level in shrimp is 20 mg/100 g. The results
376 indicated that the shrimp could be consumed on the first day. Meanwhile, the ΔE value
377 was 13.6. The TVB-N level was 31.6 mg/100 g and the ΔE value of the curcumin film
378 increased to 19.8, suggesting that the shrimp was not fresh at 36 h. However, at this
379 point, the sensory evaluation of shrimp was still acceptable to the consumers. And ΔE
380 values was greater than 12, imply the color belongs to different space. Thus, the color
381 of pH indicator were more sensitive to sensory evaluation of the shrimp. Then the
382 shrimp sample had a deeper putrefaction with the increasing storage time. The curcumin
383 film showed an obvious color changes which the ΔE values were increased to 36.5 at
384 60 h. Correspondingly, TVB-N levels of shrimp were 56.8 mg/100 g. The color of the
385 film induced by the increasing TVB-N levels and the correlation were also established
386 between the TVB-N level and the ΔE value:

$$387 \quad y = -0.0066x^2 + 1.1107x - 6.4409 \quad R^2 = 0.9731 \quad (4)$$

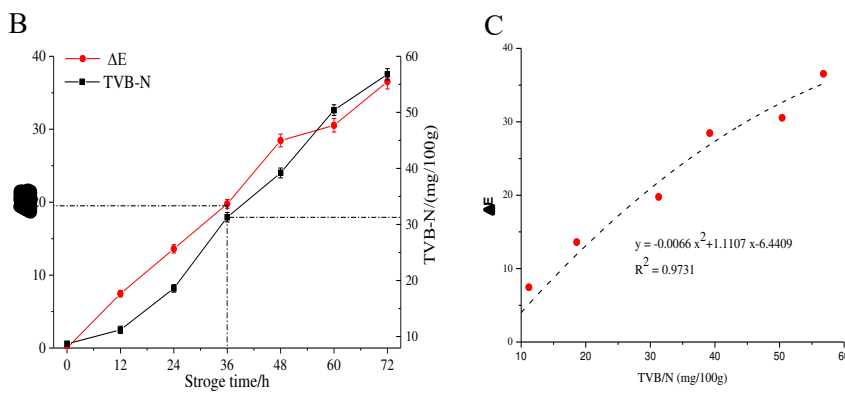
388 The positive correlation was observed between the changed color and the TVB-
389 N level with a coefficient of 0.97. Maybe this low robustness of data could be improved

390 in future studies by using some more data analysis. The correlation was responding to
 391 the ΔE value and TVB-N level of packaging and then providing information of shrimp
 392 real-time status for consumers.

393



394



395

396

397

398

399

400

401

402

Fig. 7. (A) Images of CAP2 film with red character “JU” of the shrimp from fresh to spoilage; (B) Images of CAP2 film with red characters imprint of the shrimp from fresh to spoilage; (C) The correlation between TVB-N of the shrimp and ΔE values of the curcumin film

Table S2 The GC-MS analysis results of freshness shrimp volatile compound

Number	Retention time	Compounds	Area%
1	6.97	Hexane	1.97%
2	9.86	Cyclotrisiloxane	8.23%
3	13.38	Cyclotetrasiloxane	4.11%
4	15.54	Toluene	3.43%
5	18.07	Cyclopentasiloxane	4.54%
6	27.63	Trimethylsilyl	1.02%
7	30.02	Cyanocyclohexene	2.26%
8	31.83	Indole	31.87%
9	31.87	Indole	27.92%
10	32.55	Oxime-, methoxy-phenyl	14.65%

403

404

405

Table S3 The GC-MS analysis results of spoilage volatile compound

Number	Retention time	Compounds	Area%
1	6.77	Trimethylamine	6.34%
2	7.4	Methanethiol	1.67%
3	8.21	Dimethyl sulfide	0.39%
4	9.26	Acetone	1.86%
5	11.76	Cyclopentasiloxane	0.40%
6	11.96	Methylene Chloride	0.20%
7	12.79	Heptane	0.24%
8	15.51	Toluene	0.75%
9	15.76	Ethanethioic acid,	1.97%
10	16.63	sulfuretted hydrogen	3.46%
11	18.05	Cyclopentasiloxane	2.10%
12	20.52	1-Butanol, 3-methyl	2.13%
13	21.69	Cyclohexasiloxane	2.46%
14	25.05	2-Octanol	44.40%
15	25.57	2-Nonanone	0.29%
16	25.81	Dimethyl trisulfide	0.89%
17	26.81	Acetic acid	1.73%
18	34.21	Cyclohexasiloxane	1.97%
19	37.82	Phenol	26.74%

406

407

408 **4. Conclusion**

409 In this study, the visual indicator was successfully developed and then provided an
410 effective non-destructive means for shrimp freshness. The characters “JU” were
411 successfully printed on a hydrogel film by using an electrochemical analyzer. The SEM
412 images revealed that at lower content, curcumin was well-distributed in the film-
413 forming materials. The color stability results indicated that the curcumin films
414 possessed higher color stability within 14 days which ΔE values was 3.93% at 4 °C.
415 And the response sensitivity of curcumin film showed visible color changes in the
416 presence of ammonia. Finally, the changed color from yellow to red/orange of curcumin
417 film was easily recognizable by the naked eyes with the deterioration process of the
418 shrimp. Also a positive correlation was established between the TVB-N of shrimp and
419 the ΔE value with a coefficient of 0.97. Future studies should focus on the imprint
420 characters of the hydrogel film that can be used as a sensor under an acidic environment
421 (i.e. red back to yellow) and curcumin as a reference to explore a new multifunctional
422 intelligent packaging in food packaging systems. These intelligent systems will help
423 improve food safety and shelf life for consumers and producers.

424 **Acknowledgment**

425 The authors gratefully acknowledge the Project supported by the National Natural
426 Science Foundation of China (Grant No. 31671844, 31601543), Project supported the
427 National Key research and Development Program of China (Grant No. 2018YFD
428 0400800), Project supported by the Natural Science Foundation of Jiangsu province,

429 China (Grant No. BK20180865). Project of Faculty of Agricultural Equipment of
430 Jiangsu University. We also would like to thank our colleagues in School of Food and
431 Biological Engineering who provided assistance in this study.

432 **Declarations of interest**

433 All authors declare that they have no conflicts of interest.

434 **References**

435 Cano, A.I., Cháfer, M., Chiralt, A., González-Martínez, C., (2015). Physical and
436 microstructural properties of biodegradable films based on pea starch and PVA. *Journal*
437 *of Food Engineering* 167(49), 59-64.

438 doi:<https://doi.org/10.1016/j.jfoodeng.2015.06.003>

439 Choi, I., Lee, J.Y., Lacroix, M., Han, J., (2017). Intelligent pH indicator film
440 composed of agar/potato starch and anthocyanin extracts from purple sweet potato.
441 *Food Chemistry* 218, 122-128. doi:<https://doi.org/10.1016/j.foodchem.2016.09.050>

442 Ebrahimi Tirtashi, F., Moradi, M., Tajik, H., Forough, M., Ezati, P., Kuswandi, B.,
443 (2019). Cellulose/chitosan pH-responsive indicator incorporated with carrot
444 anthocyanins for intelligent food packaging. *International Journal of Biological*
445 *Macromolecules* 136, 920-926. doi:<https://doi.org/10.1016/j.ijbiomac.2019.06.148>

446 Hazzah, H.A., Farid, R.M., Nasra, M.M.A., Hazzah, W.A., El-Massik, M.A.,
447 Abdallah, O.Y., (2015). Gelucire-Based Nanoparticles for Curcumin Targeting to Oral
448 Mucosa: Preparation, Characterization, and Antimicrobial Activity Assessment. *Journal*
449 *of Pharmaceutical Sciences* 104(11), 3913-3924.

450 doi: <https://doi.org/10.1002/jps.24590>

451 Huang, X., Li, Z., Zou, X., Shi, J., Elrasheid Tahir, H., Xu, Y., Zhai, X., Hu, X.,
452 (2019). A low cost smart system to analyze different types of edible Bird's nest
453 adulteration based on colorimetric sensor array. *Journal of Food and Drug Analysis*
454 27(4), 876-886. doi:<https://doi.org/10.1016/j.jfda.2019.06.004>

455 Huang, X., Zou, X., Zhao, J., Shi, J., Li, Z., Shen, T., (2015). Monitoring the
456 biogenic amines in Chinese traditional salted pork in jelly (Yao-meat) by colorimetric
457 sensor array based on nine natural pigments. *International Journal of Food Science &*
458 *Technology* 50(1), 203-209. doi: <https://doi.org/10.1111/ijfs.12620>

459 Kara, Ş., Erçelebi, E.A., (2013). Thermal degradation kinetics of anthocyanins and
460 visual colour of Urmu mulberry (*Morus nigra* L.). *Journal of Food Engineering* 116(2),
461 541-547. doi:<https://doi.org/10.1016/j.jfoodeng.2012.12.030>

462 Kuorwel, K.K., Cran, M.J., Sonneveld, K., Miltz, J., Bigger, S.W., (2013).
463 Migration of antimicrobial agents from starch-based films into a food simulant. *LWT -*

464 Food Science and Technology 50(2), 432-438.
 465 doi:<https://doi.org/10.1016/j.lwt.2012.08.023>

466 Kuswandia, B., Restyana, A., Abdullah, A., Heng, L.Y., Ahmad, M., (2012). A
 467 novel colorimetric food package label for fish spoilage based on polyaniline film. Food
 468 Control 25(1), 184-189. doi:<https://doi.org/10.1016/j.foodcont.2011.10.008>

469 Li, X., Zhou, Y., Jiang, Q., Yang, H., Pi, D., Liu, X., Gao, X., Chen, N., Zhang, X.,
 470 (2019). Virulence properties of *Vibrio vulnificus* isolated from diseased zoea of
 471 freshness shrimp *Macrobrachium rosenbergii*. Microbial Pathogenesis 127, 166-171.
 472 doi:<https://doi.org/10.1016/j.micpath.2018.12.002>

473 Liu, J., Wang, H., Wang, P., Min, G., Jiang, S., Li, X., Jiang, S., (2018). Films based
 474 on κ -carrageenan incorporated with curcumin for freshness monitoring. Food
 475 Hydrocolloids 83, 134-142. doi:<https://doi.org/10.1016/j.foodhyd.2018.05.012>

476 Liu, Y., Cai, Y., Jiang, X., Wu, J., Le, X., (2016). Molecular interactions,
 477 characterization and antimicrobial activity of curcumin–chitosan blend films. Food
 478 Hydrocolloids 52, 564-572. doi:<https://doi.org/10.1016/j.foodhyd.2015.08.005>

479 Luo, N., Varaprasad, K., Reddy, G.V.S., Rajulu, A.V., Zhang, J., (2012).
 480 Preparation and characterization of cellulose/curcumin composite films. Rsc Advances
 481 2(22), 8483-8488. doi:<https://doi.org/10.1039/c2ra21465b>

482 Lyons, J.G., Geever, L.M., Nugent, M.J., Kennedy, J.E., Higginbotham, C.L.,
 483 (2009). Development and characterisation of an agar--polyvinyl alcohol blend hydrogel.
 484 J Mech Behav Biomed Mater 2(5), 485-493.
 485 doi:<https://doi.org/10.1016/j.jmbbm.2008.12.003>

486 Ma, Q., Lin, D., Wang, L., (2017a). Tara gum/polyvinyl alcohol-based colorimetric
 487 NH₃ indicator incorporating curcumin for intelligent packaging. Sensors & Actuators
 488 B Chemical 244, 759-766. doi:<https://doi.org/10.1016/j.snb.2017.01.035>

489 Ma, Q., Ren, Y., Wang, L., (2017b). Investigation of antioxidant activity and release
 490 kinetics of curcumin from tara gum/ polyvinyl alcohol active film. Food Hydrocolloids
 491 70, 286-292. doi:<https://doi.org/10.1016/j.foodhyd.2017.04.018>

492 Mangolim, C.S., Moriwaki, C., Nogueira, A.C., Sato, F., Baesso, M.L., Neto, A.M.,
 493 Matioli, G., (2014). Curcumin- β -cyclodextrin inclusion complex: stability, solubility,
 494 characterisation by FT-IR, FT-Raman, X-ray diffraction and photoacoustic
 495 spectroscopy, and food application. Food Chemistry 153(153), 361-370.
 496 doi:<https://doi.org/10.1016/j.foodchem.2013.12.067>

497 Mannozi, C., Tylewicz, U., Chinnici, F., Siroli, L., Rocculi, P., Dalla Rosa, M.,
 498 Romani, S., (2018). Effects of chitosan based coatings enriched with procyanidin by-
 499 product on quality of fresh blueberries during storage. Food Chemistry 251, 18-24.
 500 doi:<https://doi.org/10.1016/j.foodchem.2018.01.015>

501 Mohammadlinejad, S., Almasi, H., Moradi, M., (2020). Immobilization of
 502 Echium amoenum anthocyanins into bacterial cellulose film: A novel colorimetric pH
 503 indicator for freshness/spoilage monitoring of shrimp. Food Control 113, 107169.
 504 doi:<https://doi.org/10.1016/j.foodcont.2020.107169>

505 Mohan, P.R.K., Sreelakshmi, G., Muraleedharan, C.V., Joseph, R., (2012). Water

506 soluble complexes of curcumin with cyclodextrins: Characterization by FT-Raman
507 spectroscopy. *Vibrational Spectroscopy* 62(9), 77-84.
508 doi:[https://doi.org/ 10.1016/j.vibspec.2012.05.002](https://doi.org/10.1016/j.vibspec.2012.05.002)
509 Musso, Y.S., Salgado, P.R., Mauri, A.N., (2016). Smart edible films based on
510 gelatin and curcumin. *Food Hydrocolloids* 66, S0268005X16307615.
511 doi:[https://doi.org/ 10.1016/j.foodhyd.2016.11.007](https://doi.org/10.1016/j.foodhyd.2016.11.007)
512 Noronha, C.M., de Carvalho, S.M., Lino, R.C., Barreto, P.L.M., (2014).
513 Characterization of antioxidant methylcellulose film incorporated with α -tocopherol
514 nanocapsules. *Food Chemistry* 159, 529-535.
515 doi:<https://doi.org/10.1016/j.foodchem.2014.02.159>
516 Pereira, P.F., Andrade, C.T., (2017). Optimized pH-responsive film based on a
517 eutectic mixture-plasticized chitosan. *Carbohydrate Polymers* 165, 238-246.
518 doi:<https://doi.org/10.1016/j.carbpol.2017.02.047>
519 Rupesh Kumar, B., Harpreet Singh, B., Jain, V.K., Nidhi, J., (2011). Curcumin
520 nanoparticles: preparation, characterization, and antimicrobial study. *J Agric Food*
521 *Chem* 59(5), 2056-2061. doi:[https://doi.org/ 10.1021/jf104402t](https://doi.org/10.1021/jf104402t)
522 Silva-Pereira, M.C., Teixeira, J.A., Pereira-Júnior, V.A., Stefani, R., (2015).
523 Chitosan/corn starch blend films with extract from *Brassica oleraceae* (red cabbage) as
524 a visual indicator of fish deterioration. *LWT - Food Science and Technology* 61(1), 258-
525 262. doi:[https://doi.org/ 10.1016/j.lwt.2014.11.041](https://doi.org/10.1016/j.lwt.2014.11.041)
526 Soares, N.M., Mendes, T.S., Vicente, A.A., (2013). Effect of chitosan-based
527 solutions applied as edible coatings and water glazing on frozen salmon preservation –
528 A pilot-scale study. *Journal of Food Engineering* 119(2), 316-323.
529 doi:<https://doi.org/10.1016/j.jfoodeng.2013.05.018>
530 Wang, H., Hu, D., Ma, Q., Wang, L., (2016). Physical and antioxidant properties
531 of flexible soy protein isolate films by incorporating chestnut (*Castanea mollissima*)
532 bur extracts. *LWT - Food Science and Technology* 71, 33-39.
533 doi:[https://doi.org/ 10.1016/j.lwt.2016.03.025](https://doi.org/10.1016/j.lwt.2016.03.025)
534 Wu, S., Wang, W., Yan, K., Ding, F., Shi, X., Deng, H., Du, Y., (2018).
535 Electrochemical writing on edible polysaccharide films for intelligent food packaging.
536 *Carbohydrate Polymers* 186, 236. doi:[https://doi.org/ 10.1016/j.carbpol.2018.01.058](https://doi.org/10.1016/j.carbpol.2018.01.058)
537 Zhai, X., Li, Z., Shi, J., Huang, X., Sun, Z., Zhang, D., Zou, X., Sun, Y., Zhang, J.,
538 Holmes, M., Gong, Y., Povey, M., Wang, S., (2019). A colorimetric hydrogen sulfide
539 sensor based on gellan gum-silver nanoparticles bionanocomposite for monitoring of
540 meat spoilage in intelligent packaging. *Food Chemistry* 290, 135-143.
541 doi:<https://doi.org/10.1016/j.foodchem.2019.03.138>
542 Zhai, X., Li, Z., Zhang, J., Shi, J., Povey, M., (2018). Natural Biomaterial-Based
543 Edible and pH-Sensitive Films Combined with Electrochemical Writing for Intelligent
544 Food Packaging. *Journal of Agricultural and Food Chemistry* 66(48).
545 doi:[https://doi.org/ 10.1021/acs.jafc.8b04932](https://doi.org/10.1021/acs.jafc.8b04932)
546 Zhang, J., Zou, X., Zhai, X., Huang, X., Jiang, C., Holmes, M., (2019). Preparation
547 of an intelligent pH film based on biodegradable polymers and roselle anthocyanins for

548 monitoring pork freshness. *Food Chemistry* 272, 306-312.
549 doi:<https://doi.org/10.1016/j.foodchem.2018.08.041>
550 Zhou, Y., Tang, R.C., (2016). Modification of curcumin with a reactive UV
551 absorber and its dyeing and functional properties for silk. *Dyes & Pigments* 134, 203-
552 211. doi:<https://doi.org/10.1016/j.dyepig.2016.07.016>
553 Zsila, F., Bikádi, Z., Simonyi, M., (2003). Unique, pH-dependent biphasic band
554 shape of the visible circular dichroism of curcumin-serum albumin complex.
555 *Biochemical & Biophysical Research Communications* 301(3), 776-782.
556 doi:[https://doi.org/10.1016/S0006-291X\(03\)00030-5](https://doi.org/10.1016/S0006-291X(03)00030-5)
557